

On the magnetic quenching of mean-field effects in supersonic interstellar turbulence

Oliver Gressel¹★, Abhijit Bendre² and Detlef Elstner²

¹*NORDITA, KTH Royal Institute of Technology and Stockholm University, Roslagstullsbacken 23, 106 91 Stockholm, Sweden*

²*Leibniz-Institut für Astrophysik Potsdam (AIP), An der Sternwarte 16, 14482, Potsdam, Germany*

Accepted 1988 December 15. Received 1988 December 14; in original form 1988 October 11

ABSTRACT

The emergence of large-scale magnetic fields observed in the diffuse interstellar medium is explained by a turbulent dynamo. The underlying transport coefficients have previously been extracted from numerical simulations. So far, this was restricted to the *kinematic* regime, but we aim to extend our analysis into the realm of dynamically important fields. This marks an important step on which derived mean-field models rely to explain observed equipartition-strength fields. As in previous work, we diagnose turbulent transport coefficients by means of the test-field method. We derive quenching functions for the dynamo α effect, diamagnetic pumping, and turbulent diffusivity, which are compared with theoretical expectations. At late times, we observe the suppression of the vertical wind. Because this potentially affects the removal of small-scale magnetic helicity, new concerns arise about circumventing constraints imposed by the conservation of magnetic helicity at high magnetic Reynolds numbers. While present results cannot safely rule out this possibility, the issue only becomes important at late stages and is absent when the dynamo is quenched by the wind itself.

Key words: Galaxy, magnetic fields, turbulence, – MHD – methods: numerical –

1 INTRODUCTION

The presence of Galactic rotation and vertical stratification renders interstellar turbulence both inhomogeneous and anisotropic. It is well known (e.g. Krause & Rädler 1980) that, in the framework of Reynolds-averaged equations, this will lead to the emergence of mean-field effects feeding on the spatial variations of the turbulence intensity and density field. Different theoretical predictions (Rüdiger & Kitchatinov 1993; Ferrière 1998) for the leading-order effects in the *kinematic* regime have previously been tested by means of simulations (Gressel et al. 2008). We now extend this approach into the domain of dynamically important magnetic fields. The main aim of the present work is to extract the intricately non-linear dependence of the measured turbulence effects on the strength of the Lorentz force – this is usually referred to as “magnetic quenching”. The knowledge of this functional dependence is required to evolve derived mean-field models into saturation. This is important, because most observed spiral galaxies are found to harbour large-scale magnetic fields of near-equipartition strength (see Fletcher 2010, for a topical compilation). Mean-field models are required to predict global symmetries of the magnetic field (Beck et al. 1996), which is neither possible in local resolved simulations, nor in global simulations ignoring effects occurring on unresolved scales. There has been an active debate (see chapter 9 in Brandenburg & Subramanian 2005, hereafter

BS05) about severe constraints inflicted upon the saturation level of the mean-field dynamo, first addressed by Vainshtein & Cattaneo (1992). These, potentially “catastrophic”, constraints can arise as a result of the conservation of magnetic helicity at large magnetic Reynolds numbers, R_m . However, Kleeorin et al. (2002) and later Shukurov et al. (2006) have demonstrated that such constraints can be alleviated by means of magnetic helicity *fluxes*. While such fluxes are likely present in our simulations in the form of advection (cf. Gressel et al. 2008), this may be restricted to the kinematic phase. For strong fields, we indeed observe the wind advection to be quenched itself in certain cases, and this will require careful attention. In the present paper, we will however ignore this complication and focus on investigating the transition into the quenched regime. We will furthermore try to distinguish between different kinds of non-linearity that have been proposed.

2 METHODS

We employ the NIRVANA-III MHD code (Ziegler 2004) to perform direct simulations of the multi-phase interstellar medium (ISM) in a local patch ($L_x = L_y = 0.8$ kpc) of the Galaxy, but retaining the vertical structure of the disc ($z \in \pm 2.1$ kpc). The grid resolution is $\Delta = 8.3$ pc, and we combine shearing-periodic boundary conditions in the plane (Gressel & Ziegler 2007) with outflow at the vertical domain boundaries, where magnetic fields obey a normal-field condition. By means of localised injection of thermal energy, we mimic the effect of supernova explosions, thereby driving strongly

★ E-mail: oliver.gressel@nordita.org

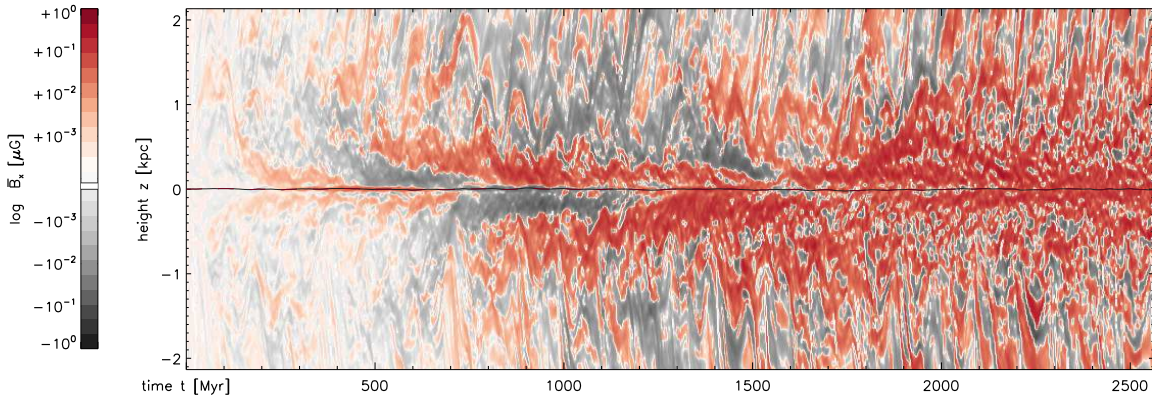


Figure 1. Space-time diagram of the radial magnetic field component. Colour coding shows the signed logarithm of the field strength. Note the evident ballistic trajectories, which are highly indicative of a Galactic fountain flow. Around $t = 1.2$ Gyr, the prevalent vertical parity changes from dipolar to quadrupolar.

supersonic turbulence. Our numerical setup is similar to our previous work but we here follow the evolution of the magnetic field into its saturation. During the course of the simulation, we employ the test-field (TF) method first introduced by Schrunner et al. (2005) to infer turbulent closure parameters such as the α effect, turbulent diamagnetism, and turbulent diffusivity. The standard flavour of this method (Schrunner et al. 2007) is now usually referred to as “quasi-kinematic” TF method (Rheinhardt & Brandenburg 2010), as it has been shown to remain fully valid into the non-kinematic regime in the absence of magnetic background fluctuations (Brandenburg et al. 2008). Since our driving is dominated by kinetic forcing and we likely remain sub-critical to exciting a small-scale dynamo (see Mantere & Cole 2012), this is warranted in our application. Whether, at higher Rm, the presence of a fluctuation dynamo will affect the evolution of the mean fields, remains open (Brandenburg, Sokoloff & Subramanian 2012).

We measure TF coefficients as a function of time, t , and vertical position, z . Due to the vertical stratification, the amplitude of the α effect significantly depends on position, as does the strength of the magnetic field. In other words, our system (unlike, e.g., forced turbulence in an unstratified triply-periodic box) has a rather poorly controlled background state and hence suffers from strong random fluctuations. Because of this, it is not straightforward to extract the quenching function. If we were to compile a naive scatter plot (as is usually done in a homogeneous setting) we are bound to confuse variations in α caused by fluctuations in the background gradients (i.e. in $\nabla\rho$ and ∇u_{rms}^2) with the attenuation due to the non-linear quenching. To resolve this degeneracy, we have to make an assumption about the systematic variation with height. A very simple possibility is to approximate the vertical profiles by a “power series” around $z = 0$, and for reasons of simplicity, we restrict ourselves to the lowest-order variation in z . For the α effect, and for the diamagnetic pumping, γ_z , we accordingly measure linear slopes within a defined central range in z . This is guided by inspection of Fig. 3 presented in the following section. The turbulent diffusivity, η_T , of course, has a dominant even parity with respect to $z = 0$, and we accordingly apply a quadratic fit.

The vertical profiles of the magnetic and kinetic energy densities are found to be roughly bell-shaped. As a measure for the relative importance of the magnetic field, we introduce the quantity $\beta \equiv \langle \bar{B}/B_{\text{eq}} \rangle$ as their ratio; here we have used $\bar{B} \equiv |\bar{\mathbf{B}}| = (\bar{B}_R^2 + \bar{B}_\phi^2)^{1/2}$, and $B_{\text{eq}} \equiv (\mu_0\rho)^{1/2} u_{\text{rms}}$, with μ_0 the permeability of free space, and where overbars denote horizontal averages and angle brackets refer to rms values when averaging over (z, t) . We remark that the weak

vertical field, \bar{B}_z , remains constant throughout the run (a result of the periodic horizontal boundaries, conserving vertical flux), and hence does not influence the quenching function.

Due to strong fluctuations within the data, and to obtain reasonable statistics, we bin the data into larger sections, for which we infer data points $\alpha(\beta)$, $\gamma_z(\beta)$, and $\eta_T(\beta)$ via linear regression as described above. Based on these data, we then attempt to fit the commonly adopted algebraic quenching formula (see e.g. Ivanova & Ruzmaikin 1977)

$$\alpha(\beta) = \alpha_0 \frac{1}{1 + q_\alpha \beta^{p_\alpha}}, \quad (1)$$

with 3 independent parameters α_0 , q_α , and p_α in the case of $\alpha(\beta)$, and with analogous expressions for $\gamma_z(\beta)$ and $\eta_T(\beta)$, respectively. The following meanings can be ascribed to the three coefficients each: The subscript ‘0’ refers to the unquenched amplitude, while the power p determines the abruptness of the transition into the quenched regime; q , taken to the power of $-1/p$, can be interpreted as the (approximate) relative amplitude β at which the quenching sets in. The latter observation points at a potential correlation between these two parameters when fitting the data, and this is indeed confirmed for the case of $\alpha(\beta)$.

3 RESULTS

The model presented in this work is identical to model “Q4” in Gressel et al. (2008), with the exception that it is initialised with a nano-Gauss *vertical* field rather than a horizontal one.¹ The key parameters of the simulation are a supernova rate of a quarter the Galactic reference value of $\sigma_0 = 30 \text{ Myr}^{-1} \text{ kpc}^2$, a rotation rate of four times $25 \text{ km s}^{-1} \text{ kpc}^{-1}$, and background shear, $q = -1$, equivalent to a flat rotation curve. For further details, we refer the reader to the extensive description in Gressel (2009). In the present model, the inclusion of a net-vertical flux was chosen to investigate a potential contribution from the magnetorotational instability (see Piontek & Ostriker 2005; Korpi et al. 2010). We here ignore this issue and focus on the quenching behaviour. The effect of different field topologies will be discussed in a forthcoming publication.

¹ Strictly speaking, \bar{B}_z is not a seed field but an imposed field. However, it induces rms fluctuations in \bar{B}_R , and \bar{B}_ϕ which then act as seed.

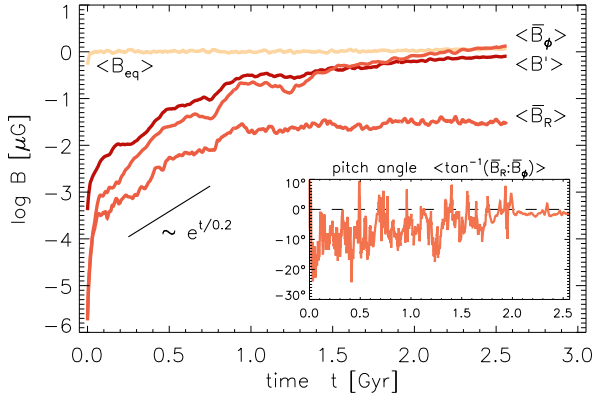


Figure 2. Time evolution of the fluctuating and regular magnetic field components, where overbars denote horizontal averages, and angle brackets refer to the rms variation within $\bar{B}_R(z)$, and $\bar{B}_\phi(z)$ at a given point in time. Note that the radial pitch angle (inset) is suppressed during saturation.

3.1 Magnetic field evolution

For our purposes, the only noticeable effect of the vertical seed field is that the growing mode takes a dipole-like symmetry with respect to the midplane, $z = 0$. This can be seen in Fig. 1, where we show the spatiotemporal structure of the horizontally averaged mean radial field. Ultimately, the quadrupolar-like vertical symmetry will dominate, but not until the parity of the field has reversed twice. Figure 1 also reveals a remarkable feature caused by the multi-phase nature of the interstellar plasma: the occurrence of return flows, tracing-out the Galactic fountain. Due to shock compression, the density is positively correlated with the magnetic field strength. As the dense clumps rain down into the Galactic potential, the frozen-in field gets dragged along. A more comprehensive analysis of the correlation of mean magnetic fields with the ISM phases will require more sophisticated methods such as the ones recently proposed by Gent et al. (2012).

If we apply a further rms average over the vertical direction, we obtain an estimate for the amplitude of the growing field, which is shown in Fig. 2 according to different constituents. The turbulent velocity u_{rms} reaches a statistically stationary state after less than 100 Myr, and with it the equipartition field $\langle B_{\text{eq}} \rangle$. The fluctuating field $\langle B' \rangle$, and the radial and azimuthal mean fields show an extended phase of exponential growth, as indicated by the straight line. After the saturation of the mean-field dynamo (evident from $\langle \bar{B}_R \rangle$ remaining constant), we observe that $\langle \bar{B}_\phi \rangle$ keeps growing due to stretching by the differential rotation. As is shown in the inset of Fig. 2, this has the consequence of a negligible radial pitch angle in the saturated state – which is at odds with observational evidence of significant pitch angles for equipartition-strength regular fields (see Beck 2012). While this behaviour is characteristic for dynamos of the $\alpha\Omega$ type, it has been argued that the loss of pitch angle can be circumvented if the dynamo is instead saturated by a wind (Elstner et al. 2009). As we will substantiate shortly, this is not the case for the model “Q4” discussed here, but has in fact been observed at higher supernova rates (paper in preparation).

3.2 Derivation of quenching functions

We adopt the usual mean-field closure (cf. Brandenburg 2005) applicable to the local box geometry, and assume that the turbulent electromotive force $\mathcal{E}(z, t)$ can be approximated by vertical profiles of the mean horizontal magnetic field $\bar{\mathbf{B}} = (\bar{B}_R, \bar{B}_\phi)^T$, and its vertical

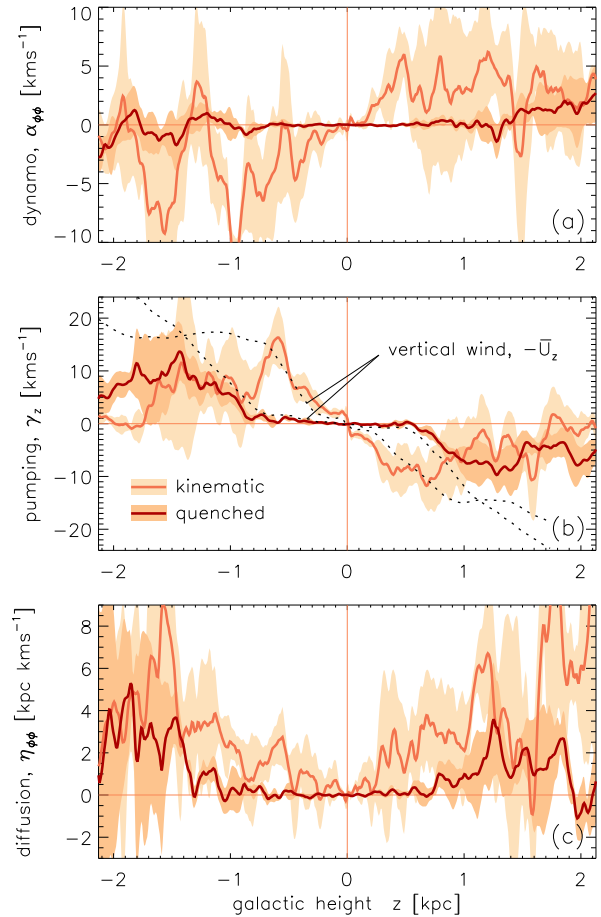


Figure 3. Time-averaged vertical profiles of the governing mean-field coefficients in the kinematic regime (light colours, $t \in [0.1, 0.3]$ Gyr), and in the fully quenched phase (dark colours, $t \in [2.3, 2.5]$ Gyr). Panels show, (a) the helical dynamo effect, $\alpha_{\phi\phi}(z)$, (b) the diamagnetic turbulent pumping, $\gamma_z(z) \equiv 0.5(\alpha_{\phi R} - \alpha_{R\phi})$, and (c) the turbulent diffusivity, $\eta_{\phi\phi}(z)$. We also overlay the mean vertical flow (dotted), mirrored for the sake of easier comparison. Note that, in both regimes, γ_z closely matches $-\bar{U}_z$ in the dynamo-active region, rendering saturation via the wind mechanism unlikely. This is in-line with the loss of pitch angle seen in Fig. 2.

gradients, i.e.,

$$\mathcal{E}_i = \alpha_{ij} \bar{B}_j - \eta_{ij} \varepsilon_{jkl} \partial_k \bar{B}_l, \quad i, j \in \{R, \phi\}, k = z. \quad (2)$$

We here focus on the relevant components of the tensors α_{ij} and η_{ij} , namely the dominant contribution $\alpha_{\phi\phi}(z)$ to the $\alpha\Omega$ dynamo, the vertical diamagnetic effect $\gamma_z(z) \equiv (\alpha_{\phi R} - \alpha_{R\phi})/2$, and the turbulent diffusivity $\eta_{\phi\phi}$. These quantities are plotted in the three panels of Fig. 3, respectively.

For each of the three effects, we show profiles at an early stage (light colours), representing the (magnetically unquenched) *kinematic* regime, and at a late time, representing the fully *quenched* regime. We observe that all three profiles are suppressed in the central region, corresponding to the belt of strong fields seen in Fig. 1. We furthermore find the mean flow \bar{U}_z to be shut-off by the emerging magnetic field, explaining the absence of quenching via the wind, and hence the low pitch angle. This is somewhat unexpected and will require careful further inspection – especially since the situation appears to change at higher supernova rate.

The central aim of the current paper is to extract quenching functions. We here restrict ourselves to run “Q4” as it presents

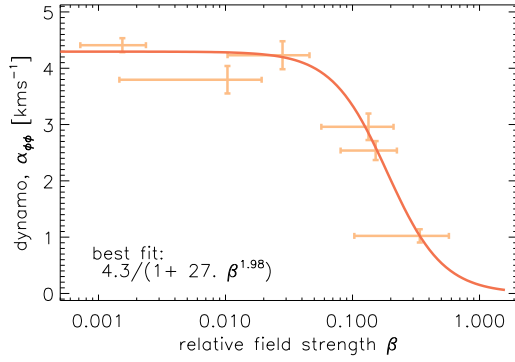


Figure 4. Amplitude of the α effect as a function of relative field strength $\beta \equiv \langle \bar{B}/B_{\text{eq}} \rangle$. Note that quenching occurs significantly below equipartition.

us with the widest range of magnetic field strengths. Comparison with other runs, however, indicates that the derived relations should be fairly universal. To disentangle the vertical variation from the magnetic field dependence, we make a model assumption on the shape of the profiles (see Sect. 2 for details). For $\alpha_{\phi\phi}(z)$ we measure the profile slope within $|z| \leq 1.33$ kpc; the resulting amplitude is plotted in Fig. 4 as a function of the relative field strength. Strictly speaking, the ordinate should have additional units kpc^{-1} , but we drop these for the sake of simplicity (and implicitly interpret the values as integral value at 1 kpc). With $p_\alpha = 1.98 \pm 0.3$, the fitted algebraic quenching function, cf. equation (1), is found in close agreement with the commonly assumed quadratic (e.g. Rogachevskii & Kleeorin 2000) dependence on β ; but note that the classic result of Moffatt (1972) and Rüdiger (1974) suggests a steeper scaling with $p_\alpha = 3$ – notably for fields *exceeding* equipartition, however. In the limit of low Rm, Sur et al. (2007) have found $p = 2$ for stochastic forcing, and $p = 3$ for steady forcing, which might provide an explanation. We, moreover, find a rather large coefficient² $q_\alpha = 27 \pm 14$. This is in fact cause for some concern as one would naively expect $q_\alpha \sim 10$, based on the scale separation $L_0/l_0 \approx 1 \text{ kpc}/0.1 \text{ kpc}$, as can be derived in the framework of dynamical quenching (see sect. 9.3.1 in BS05). A value significantly larger than this would be indicative of “catastrophic” quenching, for which one can estimate $q_\alpha \sim \text{Rm}$. In previous work, we adopted a definition of Rm based on the global box scale, arriving at a (seemingly large) value of $\text{Rm}' \equiv L^2\Omega/\eta \approx 10,000$. In the current context, it is however more realistic to base Rm on the outer scale of the turbulence, i.e. $k_f \approx 2\pi/l_0$, and a typical rms velocity, e.g. $u_{\text{rms}} \approx 25\text{--}50 \text{ km s}^{-1}$. With this new definition, we obtain a value of $\text{Rm} \equiv u_{\text{rms}}(k_f \eta)^{-1} \approx 75\text{--}125$ which is still comfortably larger than the factor appearing in the quenching expression. Another commonly used definition of Rm in this context is $\text{Rm}_T \equiv \eta_T/\eta$. With $\eta_T \approx 0.1\text{--}2.0 \text{ kpc km s}^{-1}$ in the region of interest, this makes for a poor indicator as we obtain $\text{Rm}_T \approx 15\text{--}300$, with uncertain conclusions. Nevertheless, the presence of catastrophic quenching cannot be safely ruled out here. Following the notion that alleviating helicity constraints requires a flux of helicity out of the dynamo-active region (Kleeorin et al. 2002), its occurrence would, however, be consistent with the suppression of the wind profile (see dotted line in Fig. 3) at late times. Since the wind may be the deciding factor it becomes mandatory to better understand its exact physical origin.

² As a potential caveat, we want to point out that (as speculated upon earlier) the p and q parameters are found to be correlated at the 90% level.

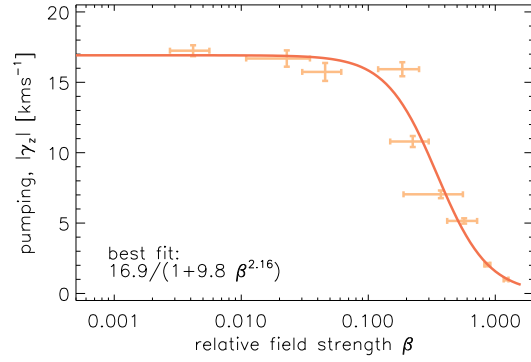


Figure 5. Same as Fig. 4, but for the amplitude $|\gamma_z|$ of the diamagnetic turbulent pumping term. Compared to $\alpha_{\phi\phi}$, the pumping appears to be quenched at somewhat higher relative field strength.

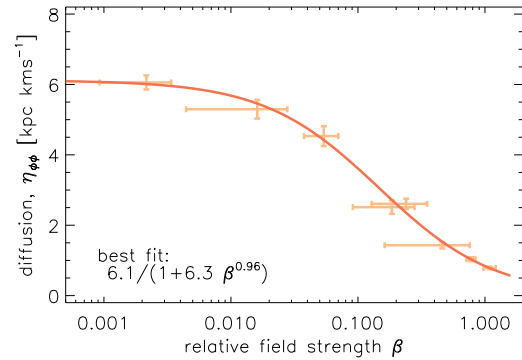


Figure 6. Same as Fig. 4, but for the turbulent diffusivity $\eta_{\phi\phi}(\beta)$.

For the diamagnetic term $\gamma_z(z)$, which is more centrally confined, we infer slopes within $|z| \leq 0.5$ kpc. Results are plotted in Fig. 5, and with $q_\gamma = 9.8 \pm 1.6$, and $p_\gamma = 2.16 \pm 0.25$, they again agree with the assumption of a quadratic dependence $\sim \beta^2$. Like for α , we are at odds with the theoretical expectations of Kitchatinov & Rüdiger (1992), who predict the same β^3 scaling for γ_z – but recall the result by Sur et al. (2007), mentioned above, which might resolve this. Because diamagnetic pumping is footed on inhomogeneity of the turbulence, but *not* on lack of mirror symmetry, it is not affected by issues of helicity conservation. This is consistent with a low value of q_γ . We moreover performed a corresponding fit for the mean flow $\bar{U}_z(\beta)$ and obtain comparable parameters. This is expected from the close correspondence between the two quantities seen in Fig. 3.

A potential buoyant contribution to the pumping (Kitchatinov & Rüdiger 1992) appears unlikely in our case as the Galaxy (unlike the solar convection zone) is only moderately stratified in density. Similarly, turbulent transport arising from small-scale magnetic fluctuations (Rädler et al. 2003) may only become important³ at higher Rm, due to small-scale dynamo action. Because we find no direct evidence for the latter, we attribute the observed attenuation to the quenching of the kinematic effect $\gamma_z \sim -1/2\nabla\eta_T$.

To conclude the results section, we present, in Fig. 6, the quenching function for the turbulent diffusivity $\eta_T(\beta)$. We note that due to background shear, the η tensor becomes anisotropic. We

³ Whether this is expected to counteract the kinematic effect is, however, dependent on rotation (cf. sect. 10.3 in BS05).

however cannot address this issue with the current data. For practical purposes, we restrict our analysis to $\eta_{\phi\phi}$. Unlike for the two preceding quantities related to the α tensor, we now find a scaling exponent closer to one, i.e. $p_\eta = 0.96 \pm 0.06$. This is in good agreement with $p_\eta = 1$, as predicted by Rogachevskii & Kleeorin (2000), and coincides with the scaling suggested⁴ by Blackman & Brandenburg (2002). Our result also agrees with the effective diffusivity (in the one-dimensional case) quoted in the line after eqn. (46) of Kitchatinov et al. (1994). Yousef et al. (2003) have derived diffusivity quenching from simulations of forced turbulence. Their results appear consistent with an assumed $p_\eta = 2$, based on which they state a best-fit value of $q_\eta = 8$.

4 DISCUSSION & CONCLUSIONS

We have provided magnetic quenching functions for the attenuation of turbulent transport coefficients in supersonic interstellar turbulence. Our results are based on realistic simulations of the stratified ISM – with the exceptions of neglecting a potential contribution from cosmic rays (CRs, Hanasz et al. 2004, 2006). Nevertheless, the obtained quenching laws represent the first quantitative result derived from such a complex scenario and will be highly useful in the global modelling of the Galactic dynamo.

Generally, the obtained results appear consistent with the picture of purely *kinematic* effects, i.e., those arising out of correlations in the fluctuations of u_{rms} . These correlations are then attenuated by the presence of a strong mean field. A key question to address in future studies is, in how far correlations in background *magnetic* fluctuations (stemming, e.g., from a small-scale dynamo) will be of importance. Such contributions have usually been ignored since they are hard to capture. On the other hand, recent studies have found that the small-scale dynamo is very hard to excite in the multi-phase ISM, which in turn challenges its importance.

Independent of these, a potential influence of additional constraints (arising from magnetic helicity conservation at high magnetic Reynolds numbers) cannot safely be excluded at the current stage. Given the considerable uncertainty in determining the related q parameter, we conclude that settling this issue will require more detailed investigation of the scaling of our result with R_m , demanding for potentially very expensive computations. It is interesting to note that, in comparable simulations, Del Sordo et al. (2012) found the influence of a wind enhanced at higher R_m , pointing to a possible solution. As far as our own simulations are concerned, we will need a thorough understanding of the conditions under which the vertical wind is attenuated as it may play a crucial role in alleviating helicity constraints. Because the inclusion of a CR component may potentially resolve this deficiency, we are nevertheless confident that the paradigm of a turbulent mean-field dynamo will prevail in explaining large-scale Galactic magnetic fields.

ACKNOWLEDGEMENTS

We are grateful to Axel Brandenburg for giving insightful comments on an earlier draft of this manuscript. We also thank Günther Rüdiger for discussing his analytical findings, and the anonymous referee for providing useful comments. This work used the NIRVANA code version 3.3, developed by Udo Ziegler at the Leibniz-Institut für Astrophysik Potsdam (AIP). Computations were performed on

the babel compute cluster at the AIP. This project is part of DFG research unit 1254.

REFERENCES

- Beck R., 2012, *Space Sci. Rev.*, 166, 215
 Beck R., Brandenburg A., Moss D., Shukurov A., Sokoloff D., 1996, *ARA&A*, 34, 155
 Blackman E. G., Brandenburg A., 2002, *ApJ*, 579, 359
 Brandenburg A., 2005, *AN*, 326, 787
 Brandenburg A., Rädler K., Rheinhardt M., Subramanian K., 2008, *ApJ*, 687, L49
 Brandenburg A., Sokoloff D., Subramanian K., 2012, *Space Sci. Rev.*, p. 57
 Brandenburg A., Subramanian K., 2005, *Phys. Rep.*, 417, 1
 Del Sordo F., Guerrero G., Brandenburg A., 2012, *ArXiv e-prints*
 Elstner D., Gressel O., Rüdiger G., 2009 Vol. 259 of *IAU Symp.*, Galactic dynamo simulations. pp 467–478
 Ferrière K., 1998, *A&A*, 335, 488
 Fletcher A., 2010, in Kothes R., Landecker T. L., Willis A. G., eds, Vol. 438 of *ASP Conference Series*. pp 197–210
 Gent F. A., Shukurov A., Fletcher A., Sarson G. R., Mantere M. J., 2012, *ArXiv e-prints*
 Gressel O., 2009, PhD thesis, University of Potsdam, (2009)
 Gressel O., Elstner D., Ziegler U., Rüdiger G., 2008, *A&A*, 486, L35
 Gressel O., Ziegler U., 2007, *CoPhC*, 176, 652
 Gressel O., Ziegler U., Elstner D., Rüdiger G., 2008, *AN*, 329, 619
 Hanasz M., Kowal G., Otmianowska-Mazur K., Lesch H., 2004, *ApJ*, 605, L33
 Hanasz M., Otmianowska-Mazur K., Kowal G., Lesch H., 2006, *AN*, 327, 469
 Ivanova T. S., Ruzmaikin A. A., 1977, *Soviet Ast.*, 21, 479
 Kitchatinov L. L., Pipin V. V., Rüdiger G., 1994, *AN*, 315, 157
 Kitchatinov L. L., Rüdiger G., 1992, *A&A*, 260, 494
 Kleeorin N., Moss D., Rogachevskii I., Sokoloff D., 2002, *A&A*, 387, 453
 Korpi M. J., Käpylä P. J., Väisälä M. S., 2010, *AN*, 331, 34
 Krause F., Rädler K. H., 1980, *Mean-field magnetohydrodynamics and dynamo theory*. Oxford: Pergamon Press, 1980
 Mantere M. J., Cole E., 2012, *ApJ*, 753, 32
 Moffatt H. K., 1972, *Journal of Fluid Mechanics*, 53, 385
 Piontek R. A., Ostriker E. C., 2005, *ApJ*, 629, 849
 Rädler K.-H., Kleeorin N., Rogachevskii I., 2003, *Geophysical and Astrophysical Fluid Dynamics*, 97, 249
 Rheinhardt M., Brandenburg A., 2010, *A&A*, 520, A28+
 Rogachevskii I., Kleeorin N., 2000, *Phys. Rev. E*, 61, 5202
 Rüdiger G., 1974, *AN*, 295, 275
 Rüdiger G., Kitchatinov L. L., 1993, *A&A*, 269, 581
 Schrunner M., Rädler K.-H., Schmitt D., Rheinhardt M., Christensen U., 2005, *AN*, 326, 245
 Schrunner M., Rädler K.-H., Schmitt D., Rheinhardt M., Christensen U. R., 2007, *GApFD*, 101, 81
 Shukurov A., Sokoloff D., Subramanian K., Brandenburg A., 2006, *A&A*, 448, L33
 Sur S., Subramanian K., Brandenburg A., 2007, *MNRAS*, 376, 1238
 Vainshtein S. I., Cattaneo F., 1992, *ApJ*, 393, 165
 Yousef T. A., Brandenburg A., Rüdiger G., 2003, *A&A*, 411, 321
 Ziegler U., 2004, *JCoPh*, 196, 393

⁴ Note that this value is not derived from a quenching function but emerges when modelling an $\alpha\Omega$ dynamo and comparing it to direct simulations.

This paper has been typeset from a \TeX/L\^AT\^EX file prepared by the author.